

## EXPLORING INTRACRANIAL ANEURYSM INSTABILITY MARKERS TO IMPROVE DISEASE MODELING

Nicolas Dupuy<sup>1</sup>, Norman Juchler<sup>2</sup>, Sandrine Morel<sup>1,3</sup>, Brenda R. Kwak<sup>3</sup>,  
Sven Hirsh<sup>2</sup> and Philippe Bijlenga<sup>1</sup>

<sup>1</sup>Neurosurgery Division, Department of Clinical Neurosciences, Geneva University Hospital and Faculty of Medicine, Geneva, Switzerland, nicolas-dupuy1@hotmail.fr, sandrine.morel@hcuge.ch, philippe.bijlenga@hcuge.ch

<sup>2</sup>Institute of Applied Simulation, Zurich University of Applied Sciences, Wädenswil, Switzerland, juch@zhaw.ch, hirc@zhaw.ch

<sup>3</sup>Department of Pathology and Immunology, Faculty of Medicine, University of Geneva, Geneva, Switzerland, sandrine.morel@unige.ch, brenda.kwakchanson@unige.ch

### SUMMARY

Intracranial aneurysm (IA) shape is proposed to be a predicting factor of rupture. In this study, using 3D-angiographies, surgical and histological images, we ranked 11 IAs according to different characteristics (homogeneity, aspect and thickness), and correlations between the different ranking systems were investigated. We showed positive correlations between IA morphology (normalized total Gaussian curvature, GLN) and wall aspect ranking, and between GLN and histology ranking. Correlations between increased GLN, inhomogeneity of IA wall aspect and thickness were shown. This exploratory study supports the GLN in its ability to quantify IA shape and to be used as an IA wall feature predictor.

**Key words:** *intracranial aneurysm, morphology, wall aspect, wall thickness*

### 1 INTRODUCTION

Intracranial aneurysm (IA), which is a deformation and enlargement of the arterial lumen, affects 2-3% of the general population [1, 2]. IA rupture leads to subarachnoid hemorrhage (SAH) resulting in severe disability and death in more than 35% of the cases [3, 4]. Rupture risk estimation of IAs relies mostly on IA localization, size and irregularity of the aneurysmal dome [5, 6]. IA shape has been proposed to be a highly relevant factor to estimate IA risk of rupture [7, 8], but its objective assessment is complex. This study focuses on the quantitative characterization of IA shape based on normalized total Gaussian curvature (GLN: measure for the total Gaussian curvature of the IA dome normalized by the total curvature of a sphere with equal volume), which has been shown to be a good proxy for overall “irregularity” of the aneurysm geometry [9]. A previous study demonstrated that GLN is more effective in discriminating IA rupture than the size of the aneurysmal dome [10].

IA wall remodeling and degeneration leading to rupture have been extensively investigated during the last years and demonstrated the involvement of inflammatory cells, phenotypic modulation of smooth muscle cells, loss of endothelial cells, modifications in extracellular matrix composition, lipid accumulation, and calcification [11, 12]. Recently, we described that wall thickness heterogeneity was more often observed in ruptured IAs than in unruptured IAs [13]. Previously, by performing a semiquantitative analysis on intraoperative video microscopy, Kadasi *et al.* showed that wall thickness distribution correlated with both patient gender and aneurysm size [14].

In the present study, we explored associations between IA dome morphology based on 3D-angiography images and IA wall aspect ranked on surgical images and IA wall thickness measured on histological sections. Our aim is to provide a model of disease progression linking histology, direct observation of the IA during surgery and shape to improve IA rupture risk estimation for a better personalized clinical management.

## 2 METHODOLOGY

### 2.1 Patient data

This pilot study represents a retrospective analysis of prospectively collected data from patients with the following inclusion criteria: 1) acceptance and signature of consent forms; 2) patients older than 18 years; 3) having a saccular IA; 4) IA images obtained by 3D rotational angiography and filmed or imaged during the surgery; 5) IA surgical resection; 6) IA histology available. This study is in accordance with the Helsinki Declaration of the World Medical Association and was approved by the Cantonal Ethics Commission for Research on Human Beings, Geneva, Switzerland (@neurIST, NAC 07-056, PB\_2018-0073) [15]. Eleven IAs were retrieved from the @neurIST cohort.

### 2.2 Segmentation and morphology classification

Before the surgical intervention, a preoperative 3D rotational angiography was performed for diagnostic purposes. For each case, the IA and surrounding vessels lumen were segmented using an in-house tool based on MATLAB 2019a (Mathworks, Massachusetts, USA) or the BrainLab® program iplanner®. All segmentations were converted into surface meshes and stored as virtual 3D objects in STL file format [8]. The surface meshes were used to calculate GLN, and IAs were ranked from the smallest to the largest GLN.

### 2.3 IA wall aspect classification

During surgery, images and videos were taken to assess the aneurysm dome wall aspect (WA) defined as the microscopic view of the dome during the surgery. WA was classified as homogeneous or heterogeneous and categorized in thin (red), intermediate (pink), thick (white), fatty (yellow) or calcified (ivory) according to the color seen on the images (Figure 1). The area of the different WA categories was calculated using Fiji® (version 2.0.0-rc-69/1.52n). All IAs were classified by predominant WA and according to the proportions of visible dome area by WA types, and ranked from the most homogeneous to the most heterogeneous.

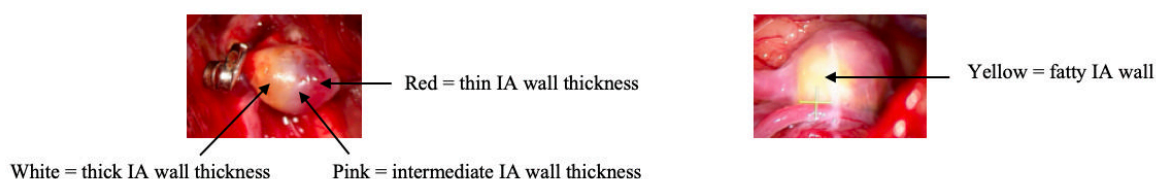


**Figure 1.** Representative examples of the IA wall aspect classification

### 2.4 IA histology classification

After clipping, IA domes were fixed in Formol, embedded in paraffin, sectioned and stained for haematoxylin and eosin, as previously described [12]. Sections were processed according to previously established protocols [12, 13]. IA wall thickness was measured using the software MATLAB 2019a (Mathworks, Massachusetts, USA), and the Gaussian curves from IA thickness frequency distribution were obtained as previously described [13]. These parameters were put together to rank IA based on thickness homogeneity and thickness values.

### 2.5 Statistics

The rankings were compared by computing non-parametric Spearman correlation coefficients. We also report p-values of a two-sided significance test under the null hypothesis that two predictors are uncorrelated. The significance level for all tests was set to 5%. Six rankings were compared: rankings from the beauty classification for 3D morphology, the WA and the histology, and the rankings from the GLN, the WA proportion and the histological dome thickness.

## 3 RESULTS AND CONCLUSIONS

### 3.1 Patients and IA characteristics

The mean age of the patients was  $58.8 \pm 14.4$  years. 7 patients were female (63.6%). 6 patients harboring multiples IAs (54.5%). 7 IAs were unruptured (63.6%). 10 IAs were located at the level of the middle cerebral artery (90.9%), and 1 at the level of the anterior cerebral artery (9.1%). The

distribution of the IAs by size was: 2–5.9 mm: 18%; 6–9.9 mm: 45%; 10–14.9 mm: 18%, 15-24.9 mm: 9%,  $\geq 25$  mm: 9%

### 3.2 IA GLN ranking

GLN is a measure for the total Gaussian curvature of the IA dome, normalized by the total curvature of a sphere with equal volume. All IAs were first classified from the smallest to the largest GLN (Figure 2).

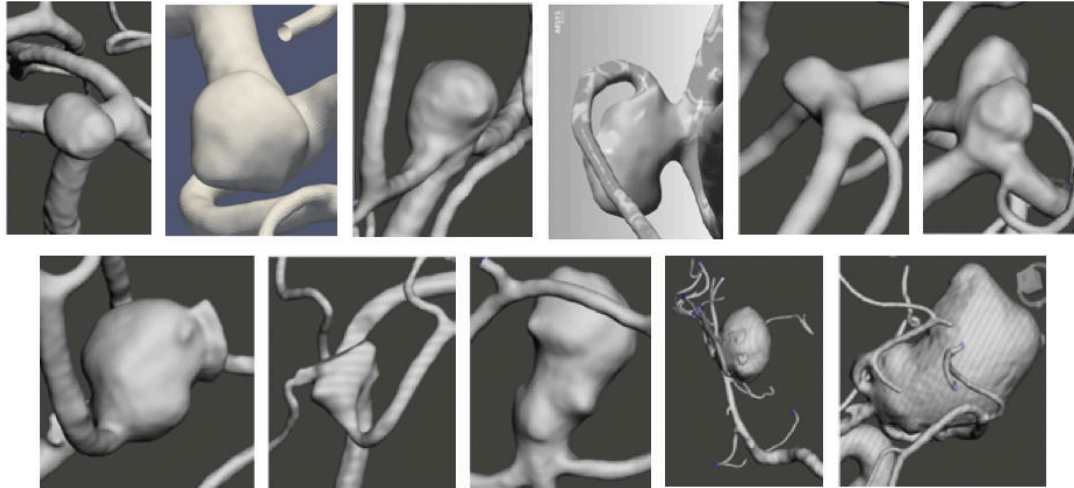


**Figure 2.** Morphology ranking according to the GLN.

The 3D images are shown from the lowest (top left) to the highest (bottom right) GLN score.

### 3.3 Correlation between GLN and WA

All IAs were classified according to the 5 pre-defined categories with respect to IA wall aspect on surgical images (Figure 1). 3 IAs (27%) had mostly a thin IA wall thickness, 5 IAs (46%) had predominantly an intermediate IA wall thickness, 2 IAs (18%) had mainly a thick IA wall thickness and 1 IA (9%) had a typical fatty IA wall.

The Spearman's coefficient of rank correlation between GLN and the WA ranking was  $\rho_{Sp}=0.717$  ( $p=0,030$ ) with a 95% confidence interval for of  $\rho_{Sp}$  0.100 to 0.936 showing a correlation between the GLN ranking method and the WA proportion ranking. Indeed, an IA described as homogeneous and thin was ranked on the top of both WA classification and GLN classification, and an IA described as heterogeneous and thick or fatty was ranked at the bottom of the WA and GLN classification. Such results confirm previous data using GLN as an effective tool for mathematical categorizing of IA shape.

### 3.4 Correlation between GLN and histology

IA wall thickness was measured for all IAs and Gaussian curves from IA thickness distribution was obtained for all IAs (Figure 3).

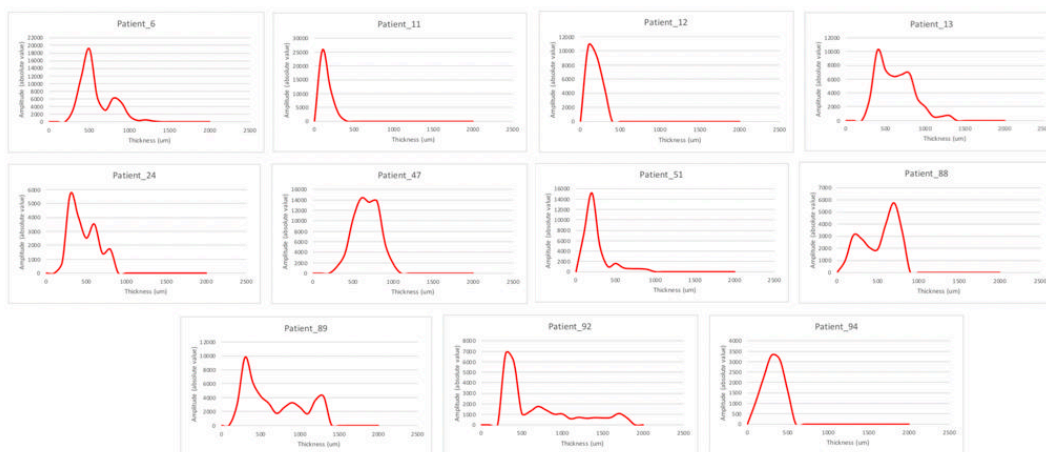


**Figure 3.** Dome wall thickness Gaussian curves for each aneurysm. Amplitude (y) is in absolute number and thickness (x) are in micrometer.

The Spearman's coefficient of rank correlation between GLN and IA wall thickness ranking was  $\rho_{Sp}=0.733$  ( $p=0.025$ ) with a 95% confidence interval for  $\rho_{Sp}$  of 0.135 to 0.940 demonstrating a correlation between the GLN ranking method and the IA wall thickness ranking method. These results suggest that IA wall thickness heterogeneity has an impact on the radiologically observable, intraluminal morphology and can be quantified by morphometric parameters such as GLN.

In this pilot study, we demonstrated a correlation between the increase in GLN and the inhomogeneity of the wall and its thickness both with the WA and histological ranking systems. Our preliminary results suggest that GLN is capable of efficiently capturing the morphological characteristics that are linked with aneurysmal wall properties. Further works are required to associate particular lumen shape attributes (blebs, lobule, thrombus) with a particular IA wall feature.

## REFERENCES

- [1] M.H. Vlak, et al., Prevalence of unruptured intracranial aneurysms, with emphasis on sex, age, comorbidity, country, and time period: a systematic review and meta-analysis. *Lancet Neurol*, 10(7): p. 626-36, 2011.
- [2] S. Morel, P. Bijlenga, and B.R. Kwak, Intracranial aneurysm wall (in)stability-current state of knowledge and clinical perspectives. *Neurosurg Rev*, 2021.
- [3] B. Schatlo, et al., Incidence and Outcome of Aneurysmal Subarachnoid Hemorrhage: The Swiss Study on Subarachnoid Hemorrhage (Swiss SOS). *Stroke*, 52(1): p. 344-347, 2021.
- [4] M.T. Lawton and G.E. Vates, Subarachnoid Hemorrhage. *N Engl J Med*, 377(3): p. 257-266, 2017.
- [5] J.P. Greving, et al., Development of the PHASES score for prediction of risk of rupture of intracranial aneurysms: a pooled analysis of six prospective cohort studies. *Lancet Neurol*, 13(1): p. 59-66, 2014.
- [6] N. Etminan, et al., The unruptured intracranial aneurysm treatment score: a multidisciplinary consensus. *Neurology*, 85(10): p. 881-9, 2015.
- [7] F.J. Detmer, et al., External validation of cerebral aneurysm rupture probability model with data from two patient cohorts. *Acta Neurochir (Wien)*, 160(12): p. 2425-2434, 2018.
- [8] N. Juchler, et al., Shape irregularity of the intracranial aneurysm lumen exhibits diagnostic value. *Acta Neurochir (Wien)*, 162(9): p. 2261-2270, 2020.
- [9] S.S. Norman Juchler, Stefan Glüge, Philippe Bijlenga, Daniel Rüfenacht, Vartan Kurtcuoglu & Sven Hirsch, Radiomics approach to quantify shape irregularity from crowd-based qualitative assessment of intracranial aneurysms. *Computer Methods in Biomechanics and Biomedical Engineering: Imaging & Visualization*, 2020.
- [10] M.L. Raghavan, B. Ma, and R.E. Harbaugh, Quantified aneurysm shape and rupture risk. *J Neurosurg*, 102(2): p. 355-62, 2005.
- [11] R. Tulamo, et al., Inflammatory changes in the aneurysm wall: a review. *J Neurointerv Surg*, 10(Suppl 1): p. i58-i67, 2018.
- [12] S. Morel, et al., Correlating Clinical Risk Factors and Histological Features in Ruptured and Unruptured Human Intracranial Aneurysms: The Swiss AneuX Study. *J Neuropathol Exp Neurol*, 77(7): p. 555-566, 2018.
- [13] J.M. Acosta, et al., Effect of Aneurysm and Patient Characteristics on Intracranial Aneurysm Wall Thickness. *Front Cardiovasc Med*, 8: p. 775307, 2021.
- [14] L.M. Kadasi, W.C. Dent, and A.M. Malek, Cerebral aneurysm wall thickness analysis using intraoperative microscopy: effect of size and gender on thin translucent regions. *J Neurointerv Surg*, 5(3): p. 201-6, 2013.
- [15] P. Bijlenga, et al., Plea for an international Aneurysm Data Bank: description and perspectives. *Neurosurg Focus*, 47(1): p. E17, 2019.